

Ab initio cluster model study of polymer–metal interactions

Mustafa Akbulut,* Walter C. Ermler and Dilhan M. Kalyon[†]

Department of Chemistry and Chemical Engineering, Stevens Institute of Technology, Hoboken, NJ 07030, USA

(Received 22 May 1997; accepted 7 June 1997)

The interactions of hydrocarbon clusters representing polyethylene with Al, Cu and Zn are studied using an ab initio atomic cluster model. Relativistic effective core potentials and full point-group symmetry were employed. A single polyethylene chain is taken to be represented by two hydrocarbon clusters, one cluster is comprised of 3 carbon and 8 hydrogen atoms, the other hydrocarbon cluster is comprised of 5 carbon and 12 hydrogen atoms. The nature of the interactions are investigated by computing potential energy surfaces, electron populations and orbital energies of systems of interest. It is found that the interaction of hydrocarbon cluster with Al is stronger than that with Cu and Zn. This study suggests the feasibility of carrying-out relativistic effective core potential calculation to numerically characterize the comparative adhesion properties of polymers with different types of metal surfaces. © 1998 Elsevier Science Ltd. All rights reserved.

(Keywords: polymer-metal; polyethylene-metal; ab initio)

INTRODUCTION

The extensive use of polymeric materials in various diverse industries has generated increased interest in the study of polymers and especially the polymer-metal interface. Since polymers have many desirable material characteristics, such as low dielectric constants and ease of processing, they are well suited for microelectronic and packaging applications.^{1,2} For example, in the microelectronic industry the polymers are often used in multilayered device systems as a dielectric material to form multilayer metallization structures. The interfaces in such devices have to be designed with certain functional characteristics, i.e., particularly favorable adhesion and chemical properties. In order to better design such interfaces it is necessary to understand the basic properties of the metal-polymer interactions.

An understanding of the polymer-metal interaction is also important for the rheology of polymers. The no-slip boundary condition assumption of continuum mechanics is violated by various rheologically complex fluids including non-Newtonian homopolymers, gels and suspensions, when certain critical conditions are exceeded in various flows.^{3–13}

Recent studies have revealed strong slip of the polymer or polymeric suspensions at the wall over a broad range of shear stresses in both capillary and parallel disk torsional flows.^{11–13} The role played by the nature of the boundary surface on the breakdown of polymer adhesion at the solid wall has been examined in series of experiments with linear low density polyethylenes.^{14,15} These investigations showed that the lack of adhesion at the polymer-metal interface is a primary cause for wall-slip effects. However, under identical flow conditions no-slip condition for ambient (with oxide overlayers) aluminum and wall slip for ambient copper dies were observed.¹⁶ This behavior was related to the greater wettability (smaller static contact angles) and greater work of adhesion values of polyethylene on ambient aluminum surfaces in comparison to ambient copper surfaces.

To be able to develop a complete microscopic understanding of the polymer-metal surface interactions, quantum mechanical investigations are necessary. In spite of the long-standing interest in studying properties of the bulk polymers^{17,18} basic studies on polymer-metal systems using quantum mechanics have been rather limited. In the past few years a number of ab initio Hartree-Fock self consistent field (SCF) investigations of the polymer-metal interfaces have been reported.^{19–22} The interaction of polyimide with different metal atoms has been studied and the results of these calculations have been used in the interpretation of X-ray

*Present address: Department of Physics, Rutgers University, Piscataway, NJ 08855, USA.

[†]To whom correspondence should be addressed, U.S. Department of Energy, ER-30/GTN, Washington, D.C. 20585, USA.

photoemission spectroscopy experiments.²³⁻²⁷ Also, to study polymer-particle and polymer-surface interactions, cluster model calculations for the interaction of polyoxymethylene fragments with ammonium perchlorate and with aluminum (100) surfaces have been performed.²⁸

The computational power of supercomputers, and the use of ab initio pseudo-potentials that include relativistic effects and molecular point group symmetry have made rigorous ab initio calculations on very large systems possible.²⁹⁻³² Ab-initio Hartree-Fock SCF calculations for clusters containing up to 135 beryllium atoms have been performed in investigations of the nature of the change in properties in going from molecular clusters to the bulk solid.²⁹ These studies, representing some of the largest such clusters investigated using ab initio quantum chemical methods to date indicate that it is possible to successfully simulate bulk systems using large clusters of atoms.

The present study aims to study the polymer-metal interactions using ab initio quantum mechanical procedures. The interactions depend largely on intrinsic properties of the metal, such as the valence electron structure. Aluminum, copper and zinc are the metal atoms selected to demonstrate that polymer-metal interactions can indeed be numerically characterized employing the ab-initio relativistic core potential approach to compare adhesive properties of various metals with polymers. Such techniques in the future can be expanded to ambient i.e. oxidized metal surfaces to facilitate a direct comparison between experiments and theory.

Computational procedures

Since the cluster systems of interest are large, the complexity of computation was reduced through the use of pseudopotentials in the form of effective core potentials that include relativistic effects (REP) to eliminate the atomic core electrons from explicit treatment in the electronic structure calculations.^{33,34} The REP is a one-electron radially-local operator which replaces the two-electron operators corresponding to the repulsion between inner-shell electrons and between core and valence electrons in a many-electron system.

Contracted Gaussian-type functions (GTF) were employed to describe the valence electrons of the clusters. Basic sets comprised of 4 s-type, 4 p-type and 6 d-type GTFs for carbon and aluminum were optimized and contracted as (2s 2p 1 d).³⁵ For copper and zinc 4 s-type, 4 p-type and 5 d-type GTFs were optimized and contracted as (2s 1p 2d).³⁶

The number of atoms in the hydrocarbon clusters representing polyethylene was chosen to be as large as possible in order to adequately represent the extended bulk systems while, at the same time, remaining computationally tractable. Two hydrocarbon clusters were studied, $\text{H}_3\text{C}(\text{CH}_2)\text{CH}_3$ and $\text{H}_3\text{C}(\text{CH}_2)_3\text{CH}_3$, to investigate how the cluster size affects the nature of interaction between the polymer and the metal. Initially, the bulk geometry of polyethylene was used³⁷ and then a limited geometry optimization was performed. Metallic surfaces can be represented by small metal clusters or even single metal atoms.³⁸

In the present study ab-initio restricted closed-shell and open-shell Hartree-Fock theory³⁹ together with REPs were employed for the polyethylene-metal systems. The calculations were carried out on Cray Y-MP supercomputers at the Pittsburgh Supercomputing Center and the Ohio Supercomputer Center. The calculations were performed in two stages: First, the multicenter integrals involving symmetry-adapted linear combinations of contracted GTFs and the appropriate terms in the Hamiltonian were evaluated for a given cluster geometry. Second, these integrals were used to calculate restricted Hartree-Fock (RHF) wave functions and energies.

The clusters were treated using their full C_{2v} point group symmetry, which significantly reduced the number of two-electron integrals processed in the calculations.⁴⁰ As shown in Figure 1, the metal atoms were chosen to lie along the molecular axis of symmetry. The distances between the hydrocarbon cluster and the metal atoms were optimized and total energies were calculated.

Mulliken population analysis was used to deduce the nature of the interactions.⁴¹ In addition, the

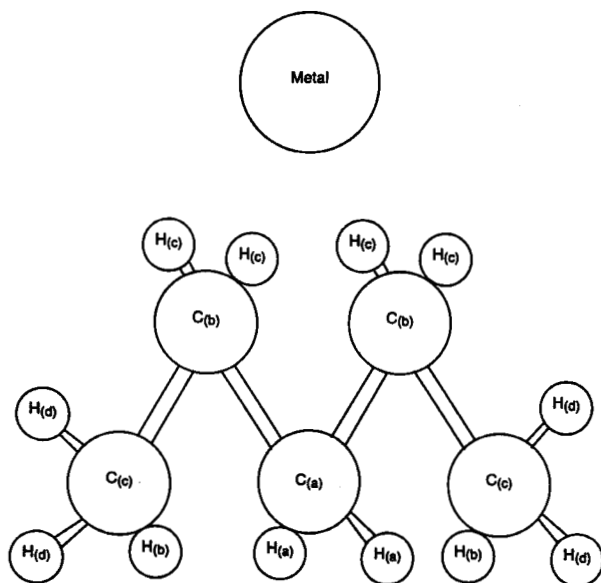


Figure 1 Metal-hydrocarbon cluster

analysis of the virtual orbitals yielded information related to the band structure of the clusters. All of the highest occupied molecular orbitals (HOMO) and lowest unoccupied orbitals (LUMO) were analyzed to determine the band width of the clusters.⁴²

RESULTS AND DISCUSSION

Hydrocarbon fragments

The calculated ground state energies of the hydrocarbon fragments which represent linear polyethylene i.e. $H_3C(CH_2)CH_3$ and $H_3C(CH_2)_3CH_3$ are given in Table 1. Population analyses of the ground states are shown in Tables 2 and 3. As expected for such a covalent bonded system, there is a small net positive charge on the hydrogen atoms and a slight net negative charge on the carbon atoms.

The orbital energies of these hydrocarbon fragments are listed in Tables 4 and 5. Using HOMOs and LUMOs the band gap values (defined as the energy difference between the HOMO and the LUMO) were calculated for these fragments. For the $H_3C(CH_2)CH_3$ the band gap is 21.2 eV and that for $H_3C(CH_2)_3CH_3$ is 14.3 eV.

Table 1 Ground state energies of $H_3C(CH_2)CH_3$ and $H_3C(CH_2)_3CH_3$

Fragment	Energy (hartrees)
$H_3C(CH_2)CH_3$	-20.931946
$H_3C(CH_2)_3CH_3$	-33.847412

Table 2 Population analysis for $H_3C(CH_2)CH_3$ (electrons/atom)

Atom ^a	Gross s	Gross p	Total
C _(a) (1)	1.28	2.49	3.77
C _(b) (2)	0.65	2.65	3.30
H _(a) (2)	1.07	0.00	1.07
H _(b) (2)	1.03	0.00	1.03
H _(c) (4)	1.04	0.00	1.04

^aNumber of symmetry-equivalent atoms shown in parentheses

Table 3 Population analysis for $H_3C(CH_2)_3CH_3$ (electrons/atom)

Atom ^a	Gross s	Gross p	Total
C _(a) (1)	1.31	2.46	3.77
C _(b) (2)	1.31	2.42	3.73
C _(c) (2)	1.27	2.84	4.10
H _(a) (2)	1.09	0.00	1.09
H _(b) (2)	0.98	0.00	0.98
H _(c) (4)	1.08	0.00	1.08
H _(d) (4)	1.02	0.00	1.02

^aNumber of symmetry-equivalent atoms shown in parentheses

Table 4 Orbital energies for $H_3C(CH_2)CH_3$ at the equilibrium geometry (hartrees)

Symmetry	HOMO	LUMO
a ₁	-0.447	0.339
a ₂	-0.579	0.533
b ₁	-0.515	0.498
b ₂	-0.506	0.379

Hydrocarbon aluminum interaction

After modeling the polyethylene by the two hydrocarbon clusters, the hydrocarbon metal interaction was investigated using both of the hydrocarbon fragments. First, the hydrocarbon-Al interaction was studied moving the Al atom along the molecular symmetry axis. Figure 2 shows the potential energy for the interaction between Al and $CH_3(CH_2)_3CH_3$. Tables 6 and 7 give the total valence energies of the molecules as a function of the distance of Al from the polyethylene fragments. Energy minima were found at 8.8 bohrs for the $CH_3(CH_2)CH_3$ -Al and 8.7 bohrs for the $CH_3(CH_2)_3CH_3$ -Al. The calculated binding energies are 0.045 and 0.046 eV for $H_3C(CH_2)CH_3$ and $H_3C(CH_2)_3CH_3$, respectively. These results show that there is no significant effect of cluster size on the binding energy.

Population analyses for these systems are shown in Tables 8 and 9. As can be seen, the weak interaction between Al and polyethylene fragments affects mainly the electron population of the hydrocarbon fragments but does not indicate chemical bonding. Only a small amount of charge transfers from the Al atom to the clusters.

Table 5 Orbital energies for $H_3C(CH_2)_3CH_3$ at the equilibrium geometry (hartrees)

Symmetry	HOMO	LUMO
a ₁	-0.363	0.178
a ₂	-0.535	0.528
b ₁	-0.510	0.479
b ₂	-0.358	0.234

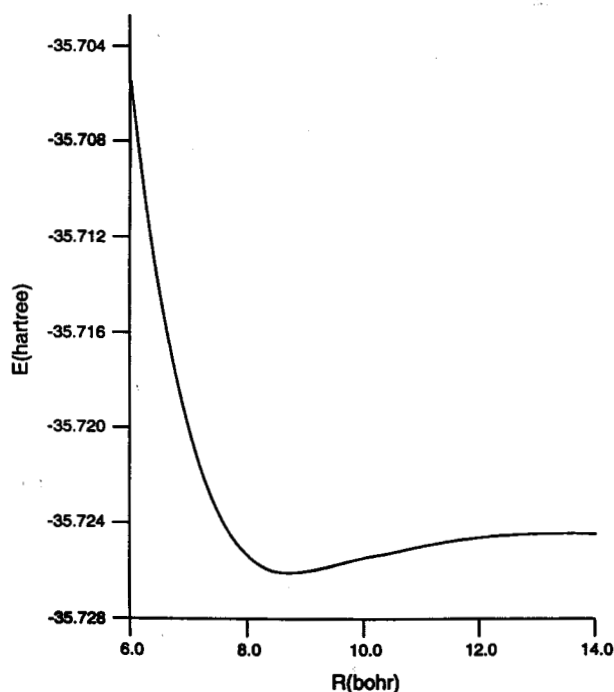


Figure 2 Potential energy curve for the Al- $CH_3(CH_2)_3CH_3$ interaction

Hydrocarbon copper interaction

A second system studied is the hydrocarbon-Cu interaction. Tables 10 and 11 show the calculated total valence energies of $H_3C(CH_2)CH_3$ -Cu and $H_3C(CH_2)_3(CH_3)$ -Cu system. These are plotted in Figure 3. The interaction of Cu with the hydrocarbon fragments results in weak interaction energies of 0.024 and 0.025 eV, respectively. These

Table 6 Total energies of $H_3C(CH_2)CH_3$ -Al

R (bohrs)	Energy (hartrees)
4.0	-22.551620
5.0	-22.713211
6.0	-22.779271
7.0	-22.803119
7.5	-22.807703
8.0	-22.809816
8.5	-22.810544
8.6	-22.810590
8.7	-22.810614
8.8	-22.810618
8.9	-22.810607
9.0	-22.810582
10.0	-22.810031

Table 7 Total energies of the $H_3C(CH_2)_3CH_3$ -Al

R (bohrs)	Energy (hartrees)
4.0	-35.475472
5.0	-35.637530
6.0	-35.700030
7.0	-35.720185
7.5	-35.723855
8.0	-35.725522
8.5	-35.726083
8.6	-35.726116
8.7	-35.726129
8.8	-35.726127
8.9	-35.726111
9.0	-35.726084
9.5	-35.725849
10.0	-35.725555

Table 8 Population analysis for $H_3C(CH_2)CH_3$ -plus Al (electrons/atom)

Atom ^a	Gross s	Gross p	Gross d	Total
Al	1.99	0.98	0.00	2.97
C _(a) (1)	1.27	2.48	0.00	3.75
C _(b) (2)	1.29	2.66	0.00	3.95
H _(a) (2)	1.06	0.00	0.00	1.06
H _(b) (2)	1.03	0.00	0.00	1.03
H _(c) (4)	1.04	0.00	0.00	1.04

^aNumber of symmetry-equivalent atoms shown in parentheses

Table 9 Population analysis for $H_3C(CH_2)_3CH_3$ plus Al (electrons/atom)

Atom ^a	Gross s	Gross p	Gross d	Total
Al	1.99	0.98	0.00	2.97
C _(a) (1)	1.31	2.45	0.00	3.76
C _(b) (2)	1.31	2.44	0.00	3.75
C _(c) (2)	1.27	2.84	0.00	4.11
H _(a) (2)	1.09	0.00	0.00	1.09
H _(b) (2)	0.99	0.00	0.00	0.99
H _(c) (4)	1.08	0.00	0.00	1.08
H _(d) (4)	1.03	0.00	0.00	1.03

^aNumber of symmetry-equivalent atoms shown in parentheses

results indicate that interaction between $H_3C(CH_2)_nCH_3$ and Cu is even weaker than that between $H_3C(CH_2)_nCH_3$ and Al. Although the

Table 10 Total energies of the $H_3C(CH_2)CH_3$ -Cu system

R (bohrs)	Energy (hartrees)
8.0	-71.106802
9.0	-71.120968
10.0	-71.121362
11.0	-71.121461
12.0	-71.121483
13.0	-71.121488
14.0	-71.121490
14.2	-71.121490
14.5	-71.121490
14.7	-71.121490
14.8	-71.121490
14.9	-71.121491
15.0	-71.121491
17.0	-71.121492

Table 11 Total energies of the $H_3C(CH_2)_3CH_3$ -Cu system

R (bohrs)	Energy (hartrees)
8.0	-84.035250
9.0	-84.036442
10.0	-84.036815
11.0	-84.036921
12.0	-84.036950
13.0	-84.036957
13.5	-84.036957
13.8	-84.036958
13.9	-84.036958
14.0	-84.036958
14.1	-84.036958
14.2	-84.036958
14.3	-84.036957
14.6	-84.036957
15.0	-84.036956
16.0	-84.036955

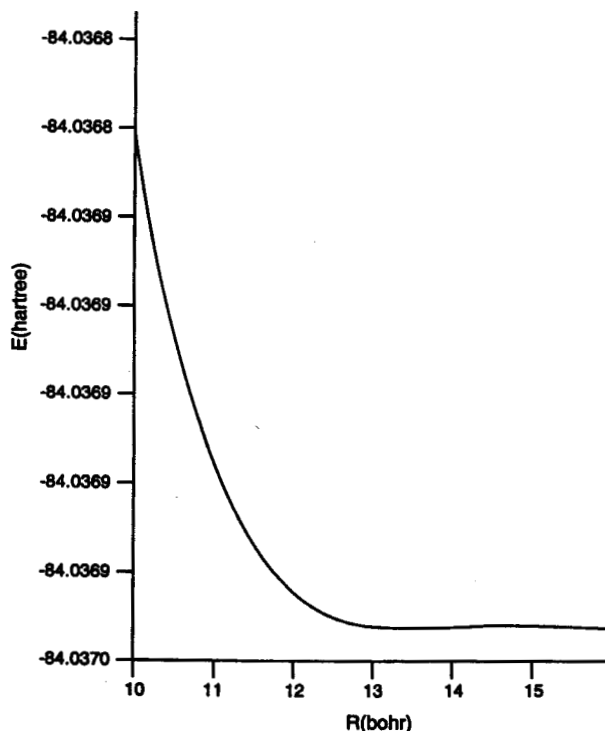


Figure 3 Potential energy curve for the Cu- $CH_3(CH_2)_3CH_3$ interaction.

presented analysis cannot be directly extended to cover oxidized metal surfaces it is interesting to note that smaller contact angle and greater work of adhesion values of polyethylene melt on ambient aluminum surfaces were observed in comparison to ambient copper.¹⁶

Population analysis for the hydrocarbon-Cu systems shows that no charge transfers from Cu to polyethylene fragments and as shown in Tables 12 and 13 and the unpaired electron of copper remains in its is orbital. Furthermore the interaction between Cu and hydrocarbon fragments does not change the electron population of hydrocarbon fragments.

Hydrocarbon zinc interaction

Finally, the hydrocarbon-Zn interaction was investigated using the cluster model. The calculated total valence energies as a function of the distance of separation of the polyethylene fragments from the Zn atom are listed in Tables 14 and 15 and are shown in Figure 4. The interaction energies for these systems were 0.00019 and 0.0002 eV, respec-

Table 12 Population analysis for the H₃C(CH₂)CH₃ plus Cu system (electrons/atom)

Atom ^a	Gross s	Gross p	Gross d	Total
Cu	1.00	0.00	10.00	11.00
C _(a) (1)	1.27	2.49	0.00	3.76
C _(b) (2)	1.29	2.65	0.00	3.94
H _(a) (2)	1.07	0.00	0.00	1.07
H _(b) (2)	1.03	0.00	0.00	1.03
H _(c) (4)	1.04	0.00	0.00	1.04

^aNumber of symmetry-equivalent atoms shown in parentheses

Table 13 Population analysis for the H₃C(CH₂)₃CH₃ plus Cu system (electrons/atom)

Atom ^a	Gross s	Gross p	Gross d	Total
Cu	1.00	0.00	10.00	11.00
C _(a) (1)	1.31	2.46	0.00	3.77
C _(b) (2)	1.31	2.42	0.00	3.73
C _(c) (2)	1.27	2.84	0.00	4.11
H _(a) (2)	1.09	0.00	0.00	1.09
H _(b) (2)	0.98	0.00	0.00	0.98
H _(c) (4)	1.08	0.00	0.00	1.08
H _(d) (4)	1.02	0.00	0.00	1.02

^aNumber of symmetry-equivalent atoms shown in parentheses

Table 14 Total energies of the H₃C(CH₂)CH₃-Zn system

R (bohrs)	Energy (hartrees)
8.5	-83.433756
9.0	-83.434136
9.5	-83.434290
10.0	-83.434342
10.5	-83.434348
10.7	-83.434353
10.9	-83.434352
11.0	-83.434351
11.5	-83.434351
12.0	-83.434351

tively. These results show that the weakest interaction for the systems studied is that of the hydrocarbon with Zn. As seen in Tables 16 and 17 no charge transfer occurs from Zn to the clusters. Unlike aluminum, the electron populations of the hydrocarbon fragments are not at all affected by their interactions with zinc. This is clear evidence of a very weak interaction between Zn and the hydrocarbon.

Overall, the reported relative behavior of hydrocarbons with different metal atoms can be explained on the basis of the comparisons of the ground state electron configurations of the metals. Both the sizes and the energies of the atomic orbitals of the metals influence the metal-hydrocarbon interactions. For example, the ground state of zinc (3d¹⁰ 4s²) behaves like a closed shell at long range.⁴³ This suggests that zinc should be inert to polyethylene as indeed observed here. On the other hand, for copper the ground state is 3d¹⁰4s¹ and this state should be more chemically active than zinc.

Table 15 Total energies of the H₃C(CH₂)₃CH₃-Zn system

R (bohrs)	Energy (hartrees)
8.0	-96.96871
9.0	-96.971535
10.0	-96.972284
11.0	-96.972437
11.8	-96.972455
12.0	-96.972455
12.2	-96.972455
12.2	-96.972455
12.5	-96.972455
13.0	-96.972454
14.0	-96.972452
15.0	-96.972452

Table 16 Population analysis for the H₃C(CH₂)CH₃ plus and Zn system (electrons/atom)

Atom ^a	Gross s	Gross p	Gross d	Total
Zn	1.99	0.00	10.00	12.00
C _(a) (1)	1.31	2.46	0.00	3.77
C _(b) (2)	1.31	2.42	0.00	3.73
C _(c) (2)	1.27	2.84	0.00	4.11
H _(a) (2)	1.09	0.00	0.00	1.09
H _(b) (2)	0.98	0.00	0.00	0.98
H _(c) (4)	1.08	0.00	0.00	1.08
H _(d) (4)	1.02	0.00	0.00	1.02

^aNumber of symmetry-equivalent atoms shown in parentheses

Table 17 Population analysis for the H₃C(CH₂)₃CH₃ plus and Zn system (electrons/atom)

Atom ^a	Gross s	Gross p	Gross d	Total
Zn	2.0	0.00	10.00	12.00
C _(a) (1)	1.31	2.46	0.00	3.77
C _(b) (2)	1.31	2.42	0.00	3.73
C _(c) (2)	1.27	2.84	0.00	4.11
H _(a) (2)	1.09	0.00	0.00	1.09
H _(b) (2)	0.98	0.00	0.00	0.98
H _(c) (4)	1.08	0.00	0.00	1.08
H _(d) (4)	1.02	0.00	0.00	1.02

^aNumber of symmetry-equivalent atoms shown in parentheses

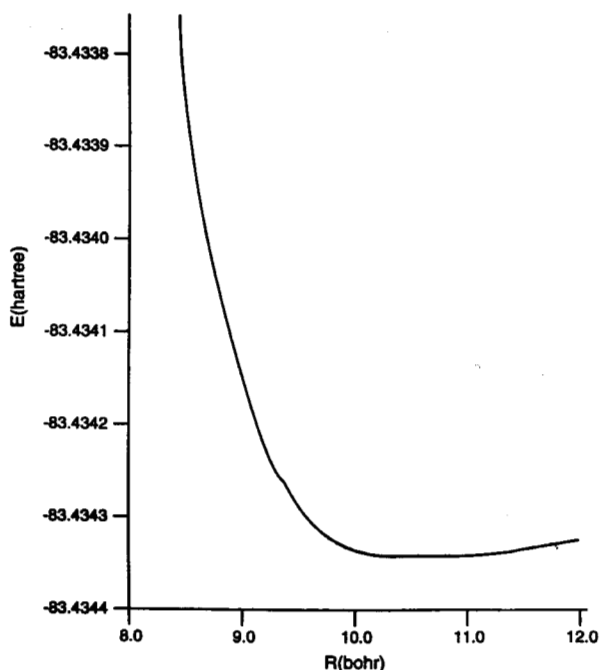


Figure 4 Potential energy curve for the Zn-CH₃(CH₂)₃CH₃ interaction

CONCLUSIONS

Polymer-metal interactions have been studied using ab initio cluster models. Metals combined with two hydrocarbon clusters representing linear polyethylene involving different number of atoms give similar results. This indicates that using clusters to investigate the polymer-metal interactions can be a valuable technique.

All of the calculations show that, no bonding occurs between the three metals and the two hydrocarbon clusters. The calculations also indicate that there is a stronger interaction between Al and the hydrocarbons than either Cu or Zn in line with the expectations arising from the differences involved in the ground state electron configuration of the metal atoms. The results of these quantum mechanical investigations are very encouraging for the future elucidation of adhesion phenomena in general, especially the slip and adhesion effects at oxidized metal surfaces.

ACKNOWLEDGEMENTS

This research was supported in part by a grant from the National Science Foundation (CHE8912674). The Ohio Supercomputer Center and The Pittsburgh Supercomputing Center are acknowledged for grants of Cray Y-MP time. The research was also supported by the Department of the Navy, Office of the Chief of Naval Research and by Exxon Education Foundation. The views

expressed are those of the authors and not those of the Government of the United States.

REFERENCES

1. Chou, N. J. and Tang, C. H., *J. Vac. Sci. Technol.*, 1984, **A2**, 751.
2. Burkstand, J. M., *J. Appl. Phys.*, 1981, **52**, 4795.
3. Atwood, B. T. and Schowalter, W. R., *Rheol. Acta*, 1989, **28**, 134.
4. Jiang, T. Q., Young, A. C. and Metzner, A. B., *Rheol. Acta.*, 1986, **25**, 397.
5. White, J. L., Han, M. H., Nakajima, N. and Broskowski, R., *J. Rheol.*, 1991, **35**, 167.
6. Kraynik, A. M. and Schowalter, W. R., *J. Rheol.*, 1981, **25**, 95.
7. Cohen, Y. and Metzner, A. B., *J. Rheol.*, 1985, **29**, 67.
8. Hatzikiriakos, S. G. and Dealy, J. M., *J. Rheol.*, 1991, **35**, 497.
9. Aral, B. and Kalyon, D., *J. Rheol.*, 1994, **38**, 957.
10. Lim, F. J. and Schowalter, W. R., *J. Rheol.*, 1989, **33**, 1359.
11. Kalyon D. and Yilmazer, U., In *Polymer Rheology and Processing*, ed. A., Collyer and L., Utracki, Elsevier Applied Sci., London, 1990.
12. Yilmazer, U. and Kalyon, D., *J. Rheol.*, 1989, **33**, 1197.
13. Kalyon, D., Yaras, P., Aral B. and Yilmazer, U., *J. Rheol.*, 1993, **37**, 35-53.
14. Kalika, D. S. and Denn, M. M., *J. Rheol.*, 1987, **31**, 815.
15. Hatzikiriakos, S. G. and Dealy, J. M., *J. Rheol.*, 1992, **36**, 845.
16. Chen, Y., Kalyon D. and Bayramli, E., *J. Appl. Polym. Sci.*, 1993, **50**, 1169.
17. Andre, J. M., *Comput. Phys. Commun.*, 1970, **1**, 39.
18. Suhai, S., *J. Poly. Sci. Poly. Phys. Ed.*, 1983, **21**, 1341.
19. Ladik, L. and Suhai, S., *Int J. Quantum Chem. Biol. Symp.*, 1980, **9**, 213.
20. Rossi, A. R., Sanda, P. N., Silverman, B. D. and Ho, P. S., *Organometallics*, 1987, **6**, 80.
21. Buchwalter, L. P., Silverman, B. D., Witt L. and Rossi, A. R., *J. Vac. Sci. Technol.*, 1987, **A5**, 226.
22. Chakraborty, A. K., Davis, H. T., Tirrell, M., *J. Polym. Sci., Part A: Polymer Chem.*, 1990, **28**, 3185.
23. Silverman, B. D., Sanda, P. N., Claber, J. G., Ho, P. S. and Rossi, A. R., *J. Poly Sci. Polym. Chem.*, 1988, **26**, 1199.
24. Bartha, J. M., Hanh, P. O., LeGoues, F. and Ho, P. S., *J. Vac. Sci. Technol.*, 1986, **A3**, 1390.
25. Ho, P. S., Hanh, P. O., Bartha, J. W., Rubloff, G. W. and LeGoues, F. K., *J. Vac. Sci. Technol.*, 1985, **A3**, 739.
26. White, R. C., Haight, R., Silverman, B. D. and Ho., P. S., *Appl. Phys. Lett.*, 1987, **51**, 481.
27. Atanasoska, L. J., Stevens, G., Anderson, H., Meyer, M., Lin, Z. and Weaver, J. H., *J. Vac. Sci. Technol.*, 1987, **A5**, 3325.
28. Seel, M., Kunz, A. B. and Wadiak, D. T., *Phys. Rev.* 1988, **B37**, 8915.
29. Ross, R. B., Ermler, W. C., Kern C. W. and Pitzer, R. M., *Int. J. Quantum Chem.*, 1992, **41**, 733.
30. Sawamura, M. and Ermler, W. C., *J. Phys. Chem.*, 1990, **94**, 7805.
31. Ermler, W. C., Ross, R. B., Kern, C. W., Pitzer, R. M. and Winter, N. W., *J. Phys. Chem.*, 1988, **92**, 3042.
32. Ross, R. B., Ermler, W. C., Luana, V., Pitzer, R. M. and Kern, C. W., *Int. J. Quantum Chem.*, 1990, **39**, 225.
33. Christiansen, P. A., Ermler, W. C. and Pitzer, K. S., *Annu. Rev. Phys. Chem.*, 1985, **36**, 409.
34. Ermler, W. C., Lee, Y. S., Christiansen, P. A. and Pitzer, K. S., *Chem. Phys. Lett.*, 1981, **81**, 70.
35. Pacios, L. F. and Christiansen, P. A., *J. Chem. Phys.*, 1985, **82**, 2664.
36. Hurley, M. M., Pacios, L. F., Christiansen, P. A., Ross R. B. and Ermler, W. C., *J. Chem. Phys.*, 1986, **84**, 6840.
37. Karpfen, A. and Beyer, A., *J. Comp. Chem.*, 1984, **5**(1), 11-18.
38. Muettetries, E. L., Rhodin, T. N., Band, E., Brucker, C. F. and Pretzer, W. R., *Chem. Rev.*, 1979, **79**, 91.
39. Roothaan, C. C., *J. Rev. Mod. Phys.*, 1951, **23**, 69, *ibid*, 1960, **33**, 179.
40. Pitzer, R. M., *J. Chem. Phys.*, 1973, **58**, 3111.
41. Muliken, R. S., *J. Chem. Phys.*, 1955, **23**, 1833.
42. Hunt, W. J. and Goodard III, W. A., *Chem. Phys. Lett.*, 1969, **3**, 414.
43. Margareta, R., Blomberg, A., Siegbahn, P. E. M., Nagoshima, U. and Wennerberg, J., *J. Am. Chem. Soc.*, 1991, **113**, 424.
44. Ritter, D. and Weissshaer, J. C., *J. Am. Chem. Soc.*, 1990, **112**, 6425.
45. Nicolas G. and Barttlelet, J. C., *J. Phys. Chem.*, 1986, **90**, 2870.